Collective Motion in Selected Central Collisions of Au on Au at 150A MeV

S.C. Jeong,[1] N. Herrmann,[2] Z.G. Fan,[1] R. Freifelder,[1] A. Gobbi,[1] K.D. Hildenbrand,[1] M. Krämer,[1] J. Randrup,[1],[14] W. Reisdorf,[1] D. Schüll,[1] U. Sodan,[1] K. Teh,[1] J.P. Wessels,[1] D. Pelte,[2] M. Trzaska,[2] T. Wienold,[2] J.P. Alard,[5] V. Amouroux,[5] Z. Basrak,[13] N. Bastid,[5] I.M. Belayev,[8] L. Berger,[5] M. Bini,[6] Th. Blaich,[7] S. Boussange,[5] A. Buta,[3] R. Čaplar,[13] C. Cerruti,[11] N. Cindro,[13] J.P. Coffin,[11] R. Dona,[11] P. Dupieux,[5] J. Erö,[4] P. Fintz,[11] Z. Fodor,[4] L. Fraysse,[5] S. Frolov,[8] Y. Grigorian,[9] G. Guillaume,[11] S. Hölbling,[13] A. Houari,[11] F. Jundt,[11] J. Kecskemeti,[4] P. Koncz,[4] Y. Korchagin,[8] R. Kotte,[10] C. Kuhn,[11] M. Ibnouzahir,[5] I. Legrand,[3] A. Lebedev,[8] C. Maguire,[11] V. Manko,[9] P. Maurenzig,[6] G. Mgebrishvili,[9] J. Mösner,[10] D. Moisa,[3] G. Montarou,[5] I. Montbel,[5] P. Morel,[5] W. Neubert,[10] A. Olmi,[6] G. Pasquali,[6] M. Petrovici,[3] G. Poggi,[6] F. Rami,[11] V. Ramillien,[5] A. Sadchikov,[9] Z. Seres,[4] B. Sikora,[12] V. Simion,[3] S. Smolyankin,[8] R. Tezkratt,[11] M.A. Vasiliev,[9] P. Wagner,[11] Z. Wilhelmi,[12] D. Wohlfarth,[10] and A.V. Zhilin[8]

(FOPI Collaboration)

[1] *Gesellschaft für Schwerionenforschung, Darmstadt, Germany*
[2] *Physikalisches Institut der Universität Heidelberg, Heidelberg, Germany*
[3] *Institute for Physics and Nuclear Engineering, Bucharest, Romania*
[4] *Central Research Institute for Physics, Budapest, Hungary*
[5] *Labo de Phys. Corp., Institut National de Physique Nucleaire et de Physique des Particules–Centre National de la Recherche Scientifique, Université Blaise Pascal, Clermont-Fd., France*
[6] *Università and Istituto Nazionale di Fisica Nucleare, Florence, Italy*
[7] *Universität Mainz, Mainz, Germany*
[8] *Institute for Experimental and Theoretical Physics, Moscow, Russia*
[9] *Kurchatov Institute for Atomic Energy, Moscow, Russia*
[10] *Forschungszentrum, Rossendorf, Germany*
[11] *Centre de Recherches Nucléaires and Université Louis Pasteur, Strasbourg, France*
[12] *Institute of Experimental Physics, Warsaw University, Warsaw, Poland*
[13] *Rudjer Boskovic Institute, Zagreb, Croatia*
[14] *Lawrence Berkeley Laboratory, Berkeley, California 94701*

(Received 1 June 1993; revised manuscript received 14 April 1994)

Using the FOPI facility at GSI Darmstadt, complete data of Au on Au collisions at 150A MeV were collected for charged products (Z = 1–15) at laboratory angles $1° \leq \Theta_{lab} \leq 30°$. Central collisions were selected by applying various criteria. The kinetic energy spectra of fragments from an isolated midrapidity source are investigated in detail for center-of-mass angles $25° \leq \Theta_{c.m.} \leq 45°$. The heavy products ($Z \geq 3$) are used to determine the collective energy which is found to be at least 10A MeV.

PACS numbers: 25.70.Pq

The origin of transverse flow observed in collisions of nuclei at intermediate energies (50–1000A MeV) is at present a highly debated issue. It may involve different phenomena, e.g., (i) the release of compressional energy [1–3], (ii) momentum dependent forces [4], (iii) in-medium cross sections [5], and (iv) the thermal pressure burst [6].

For not too small impact parameters, where the presence of a reaction plane can be determined experimentally, the flow of matter was observed in plane ("side splash" [7], directivity [8]) and out of plane ("squeeze out" [9]). Mostly light charged particles (p, α) but partly also clusters ($Z \geq 3$) were measured; the latter were claimed to carry a clearer signal of the collective motion [10]. The presence of flow was deduced from transverse momentum analysis [11] and from the observed azimuthal distributions.

Little is known about flow for small impact parameters towards the very central collisions ($b \rightarrow 0$): in such a situation the reaction plane disappears, the azimuthal distributions become isotropic, and the normal flow analyses are not applicable any more. However, central collisions are particularly interesting since, for them, stopping, compression, and equilibration are expected to be largest and all the initial kinetic energy is deposited into "one source" located at midrapidity [12]: this greatly simplifies the collision dynamics, reduces surface effects, and enhances volume effects. For $b \rightarrow 0$, pronounced flow effects were predicted by hydrodynamical calculations [13] and earlier attempts to explain various data

0031-9007/94/72(22)/3468(4)$06.00

[14–16] lead to estimates as high as 40% for the compressional energy at highest density [17].

In this work we extract for the first time directly from experiment the amount of collective energy present in the exit channel of central collisions. Using the 4π detector FOPI [18] a comprehensive measurement was performed at GSI Darmstadt for the reaction Au on Au at 150A MeV. The setup consisted of a high granularity time-of-flight wall (764 scintillators), supplemented with an inner shell of thin energy-loss detectors (188 elements), covering laboratory polar angles of $1° \leq \theta_{\rm lab} \leq 30°$ over the full azimuth and allows element identification of charged particles ($Z \leq 15$) with detection thresholds increasing for $Z = 1$ to 15 from 14A to 50A MeV, respectively. The amount of collective energy is extracted from the mean kinetic energy of the heavy products ($3 \leq Z \leq 8$).

The extraction of a collective flow in central collisions depends on how well a representative event sample of central collisions can be selected by applying specific criteria. In a previous Letter [12] we have presented for the same set of data a new way to isolate an event sample of 40 mb cross section of central collisions, based on a combined multiplicity and directivity cut. While proving the existence of this midrapidity source of clusters this method is not able to prepare event samples with average impact parameters below 2 fm. In this Letter we want to address the expansion dynamics of very central collisions with the need to study the centrality dependence down to the smallest accessible impact parameters. For this purpose we use in the following the stopping variable $E_{\rm rat}$ defined by $E_{\rm rat} = \sum_i E_{\perp,i} / \sum_i E_{\parallel,i}$ [the sum runs over the forward hemisphere of the center-of-mass system (c.m.s.) for all products detected in an event]. This quantity was found to give good selectivity and due to its exponential distribution allows for a continuous variation down to azimuthally symmetric events [19–22] with vanishing directivity, thus giving access to very small impact parameters.

Cutting at a moderate value of $E_{\rm rat} > 0.8$ corresponding to an integrated cross section of 90 mb and hence to a sharp-cutoff geometrical impact parameter of $b_{\rm geo} = 1.8$ fm results in the rapidity plot of Fig. 1: it indicates the presence of a single source centered at midrapidity. We show in the following that even when including the effects of the selection criteria and the detection biases the measured kinetic energy distributions of heavy fragments can only be explained by introducing a collective flow component of at least 10A MeV.

This claim is inspired by the inspection of the invariant kinetic energy spectra in Fig. 2. It directly reveals a nonthermal component: while the hydrogen spectrum is compatible with a thermal scenario as obtained by modeling a hot single source of total system mass and total available energy by an extended FREESCO [23] simulation including Coulomb interaction [24] (dotted histograms), this model completely fails to explain the large kinetic energies of the heavier fragments. This deficiency can be cured in the framework of a simple blast scenario [3,14,22,24,25] which divides the energy into a collective and a thermal component. Assuming for simplicity a linear and isotropic profile for the collective velocity distri-

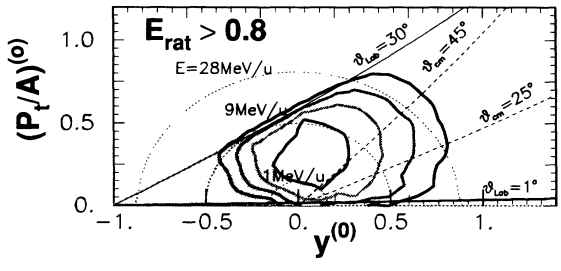

FIG. 1. Experimental rapidity plot for fragments with charge $3 \leq Z \leq 8$ for $E_{\rm rat} \geq 0.8$. Different fragments enter weighted with their respective element number. The contour lines represent cuts in invariant cross section (linear scale). The transverse momentum and rapidity scales are normalized as follows: $p_t^{(0)} = (p_t/A)/(p_{\rm pr}^{\rm c.m.}/A_{\rm pr})$ and $y^{(0)} = (y)/y_{\rm pr}^{\rm c.m.}$, respectively, where p_t and y are center-of-mass quantities; the index pr denotes projectile quantities. The solid lines indicate the detector boundary angles and the hatched area represents the energy threshold for $Z = 6$ products. The dotted circles denote constant energies per nucleon in the center of mass (1, 9, and 28A MeV, respectively).

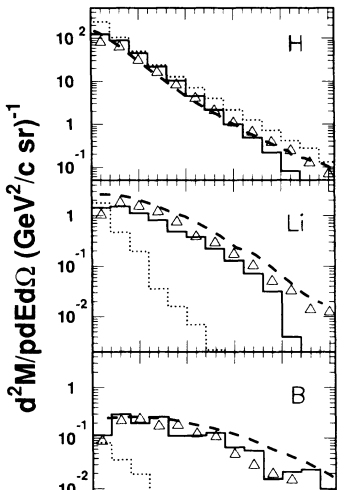

FIG. 2. Invariant kinetic energy distributions $[d^2M/(p\,dE\,d\Omega)]$ in the center of mass, normalized by the number of events for different elements $Z = 1$, 3, and 5. The rest mass of the proton is denoted by m_0 and the momentum of the products by p. The experimental data (open triangles), integrated over the c.m. angular range from 25° to 45°, have been obtained for $E_{\rm rat} \geq 0.9$. Results from the statistical model FREESCO [24] are shown by the dotted histograms. The solid histograms are obtained from a QMD simulation [2]; the dashed curves are given by a fit making use of an explosion scenario [22].

bution [1,3] the optimization of just one parameter, the average flow velocity, yields the dashed lines in Fig. 2. A flow value of $(18 \pm 2)A$ MeV describes the data best, the indicated uncertainty reflects variations when the fit is restricted to different polar angle bins.

The conjecture that the spectral shape is dominated by a radial collective flow component is, however, only convincing, if the biases of the event selection can be controlled. The comparison with a simple one-source scenario is only valid for very central collisions ($b \rightarrow 0$) which occur with vanishing probability in nature. Therefore residual anisotropies with respect to the reaction plane are unavoidable. On the $E_{\rm rat}$ scale employed in this Letter, the sideward flow has a maximum at $E_{\rm rat} \approx 0.5$ [$\langle b \rangle \approx 4$ fm, see Fig. 3(c)] with an average directed transverse flow energy of $0.8A$ MeV, decreases almost linearly with $E_{\rm rat}$ and disappears for $E_{\rm rat} \approx 1.2$ [20,21]. For the considered c.m. angular range the anisotropies of heavy clusters ($6 \leq Z \leq 8$) which display the sideward flow effects most strongly [10], are summarized in Fig. 3: The histograms in panel (b) give azimuthal distributions with respect to the reaction plane, calculated by the transverse momentum method [11], for two $E_{\rm rat}$ bins. Panel

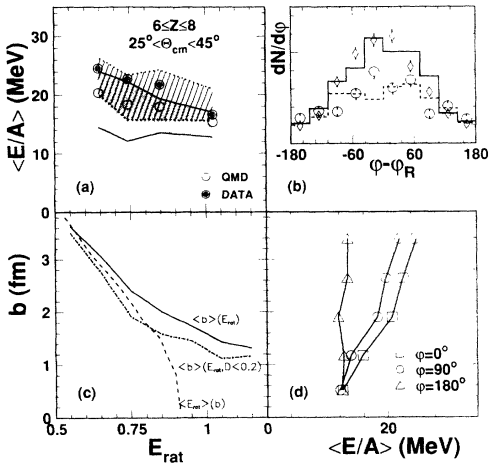

FIG. 3. Panel (a) shows for fragments with charges $6 \leq Z \leq 8$ the average kinetic energies in the angular range from 25° to 45°. Filled (open) circles represent data (QMD simulations [2]) at an azimuthal angle of 90° ± 45° with respect to the reaction plane; the upper and lower borders of the hatched (shaded) area show the corresponding values at 0° ± 45° and 180° ± 45°, respectively. Panel (b) displays for two $E_{\rm rat}$ bins, $0.7 < E_{\rm rat} < 0.8$ (solid line, diamonds) and $E_{\rm rat} > 0.9$ (dashed line, circles), the azimuthal distributions with respect to the reaction plane; histograms correspond to data, symbols to QMD simulations. Panel (c) shows the dependence of the average impact parameter as a function of $E_{\rm rat}$ (solid line), with an additional directivity cut (dash-dotted line), and the average $E_{\rm rat}$ as a function of the impact parameter (dashed line) within the QMD calculation. Panel (d) displays the average kinetic energies per nucleon as a function of the impact parameter and the azimuthal orientation within the QMD calculation.

(a) shows the variation of the mean kinetic energies per nucleon $\langle E \rangle / A$ with $E_{\rm rat}$. The dependence of the mean kinetic energies on the $E_{\rm rat}$ selection is comparatively weak: the $\langle E \rangle / A$ values decrease by less than 30% in the $E_{\rm rat}$ range considered, whereas the anisotropy of the azimuthal distribution [panel (b)] drops by a factor of 2 when $E_{\rm rat}$ changes from 0.75 to 1.

These observations can be explained in the framework of an exploding source with a nonspherical shape caused by finite values of the impact parameter. The consistency of the picture is supported by the comparison to a dynamical model calculation that allows us to study the selection and detection efficiency effects. We refer to the same QMD calculation [2] that was already used in [12] to explain the directivity selection. In its version with a hard equation of state, without momentum dependence, and with parametrized G-matrix cross sections [26] it is very successful in the $E_{\rm rat}$ distribution, the correlation of directed flow with stopping, and the clusterization [20]. For the observables discussed in Fig. 3 the model almost quantitatively predicts the azimuthal distributions [open symbols in Fig. 3(b)] as well as the difference of the mean kinetic energies for the different orientations with respect to the reaction plane [open circles and shaded area in Fig. 3(a)]. The explanation of the observed trends is offered in the lower panels of Fig. 3: the average impact parameter $\langle b \rangle$ of the event sample accessible with the $E_{\rm rat}$ selection is given by the solid line in panel (c). While $\langle b \rangle$ is monotonically decreasing with increasing $E_{\rm rat}$, for the larger $E_{\rm rat}$ values the selection efficiency is getting very small, since the average $E_{\rm rat}$ value for central collisions ($b \rightarrow 0$) in this model is 0.9 [dashed line in panel (c)]. Following the model predictions the $E_{\rm rat}$ selection, even in the tail, is limited to average impact parameters of $\langle b \rangle \geq 1.2$ fm. Impact parameters of $\langle b \rangle \approx 1$ fm would be required, however, in order to observe azimuthal symmetry as shown in terms of the average kinetic energy in panel (d). The experimentally observed mean kinetic energies displayed in panel (a) are thus still affected by noncentral reactions, but the trends visible in panels (a) and (d) indicate that the value for $b = 0$ is within the boundaries of the shaded area. The calculation also suggests that an additional directivity cut [dash-dotted line in panel (c)] would lower the average impact parameter to values where the azimuthal anisotropy in the mean kinetic energy is below 20% and the symmetric component can be extracted almost directly.

The summary of these trends for the highest $E_{\rm rat}$ bin is shown in Fig. 4 in terms of the mean kinetic energy $\langle E \rangle / A$ as a function of the fragment charge Z. The data, given by the solid line ($E_{\rm rat} > 0.9$ with $\sigma = 45$ mb) and the filled circles ($E_{\rm rat} > 0.9$ and $D < 0.2$ with $\sigma = 15$ mb) are compared to the QMD predictions applying the same cuts (dashed line and open circles). The model slightly underpredicts the experimental values by $5A$ to $2A$ MeV for fragments between $Z = 3$ and $Z = 7$. Comparison to the dotted curve representing the "ther-

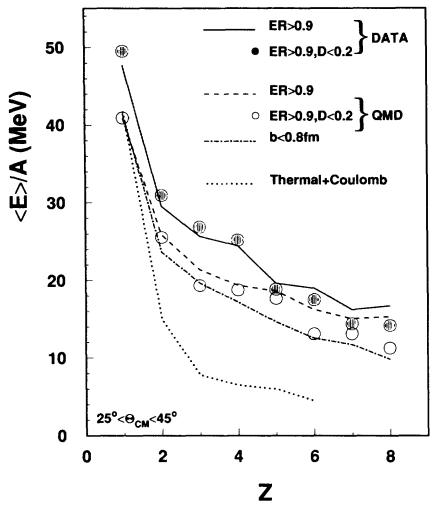

FIG. 4. Experimental results for the Z dependence of $\langle E_{\rm kin}\rangle/A$ are compared with the results from the QMD calculations [2] for $E_{\rm rat} > 0.9$ alone and an additional directivity cut. As a reference FREESCO results for a thermal scenario [24] and central QMD results are also shown.

mal + Coulomb" scenario [24] allows the conclusion that for clusters with $Z > 2$ at least $(10\pm1)A$ MeV are carried away by an azimuthally symmetric flow component. This value is obtained as an average for $6 \leq Z \leq 8$ by extrapolating the selected data sample to fully central events on the bases of the difference between QMD predictions for central ($b < 0.8$ fm, dashed-dotted line) and $E_{\rm rat}$ selected collisions. When the FREESCO predictions are subtracted from these exptrapolated energy values, the remaining energy amounts to ≈30% of the available energy in the c.m.s. The flow energies deduced by this method for lighter fragments are even higher, e.g., for $Z = 3$ one obtains $18A$ MeV. Some limitations of the current analysis should be mentioned, however: (a) the estimate of the flow energy is only valid for the angular range examined. It is very possible as the model calculation predicts that the flow energies are even larger at the larger polar angles. (b) The mass dependence of the flow pattern is not taken into account. Other analyses focusing more on the transverse part of the collective flow are currently underway to examine the phase space configuration of the expanding system [27].

In summary, during the final stage of the interaction, in central collisions of Au on Au at $150A$ MeV, a surprisingly large fraction of the initial kinetic energy, i.e., more than $10A$ MeV (≥30%), is found in the collective motion of the outstreaming matter. The kinetic energy per particle is at least an order of magnitude larger than the maximal directed transverse energy deduced from the sidewards flow and is most directly visible in the kinetic energy spectra of clusters. Coulomb repulsion and thermal motion represent a minor part in the energy balance. The small thermal energy implied as a leftover from the collective part helps us to understand the observed relatively large cluster yield but it is still too high when compared to global equilibrium statistical model predictions obtained by fitting the yield distribution [20,28]. The observed large flow component raises serious doubts whether these global thermodynamical concepts can supply the framework for even the relatively simple case of central collisions. These data should represent a valuable test bench of elaborated dynamical models, e.g., [2], [4], [6], and [29].

We acknowledge the efficient support of engineers and technical staff from the FOPI Collaboration and from the SIS accelerator division. We are grateful to J. Aichelin for supplying us with the QMD code as well as for many clarifying discussions.

[1] W. Scheid *et al.*, Phys. Rev. Lett. **32**, 741 (1974).
[2] J. Aichelin, Phys. Rep. **202**, 233 (1991); H. Stöcker *et al.*, Phys. Rep. **137**, 277 (1986).
[3] J.P. Bondorf *et al.*, Nucl. Phys. **A296**, 320 (1978).
[4] W. Cassing *et al.*, Nucl. Phys. **A545**, 123 (1992).
[5] J. Jaenicke *et al.*, Nucl. Phys. **A536**, 201 (1992).
[6] W.A. Friedman, Phys. Rev. C **42**, 667 (1990); (private communication).
[7] H.A. Gustafsson *et al.*, Phys. Rev. Lett. **52**, 1590 (1984).
[8] P. Beckmann *et al.*, Mod. Phys. Lett. A **2**, 163 (1987).
[9] D. L'Hôte, Nucl. Phys. **A488**, 457c (1988).
[10] K.G.R. Doss *et al.*, Phys. Rev. Lett. **59**, 2720 (1987).
[11] P. Danielewicz and G. Odyniec, Phys. Lett. **157B**, 146 (1985).
[12] J.P. Alard *et al.*, Phys. Rev. Lett. **69**, 889 (1992).
[13] W. Schmidt *et al.*, Phys. Rev. C **47**, 2782 (1993).
[14] P.J. Siemens and J.O. Rasmussen, Phys. Rev. Lett. **42**, 880 (1979).
[15] K.H. Kampert, J. Phys. G **15**, 691 (1989).
[16] H.W. Barz *et al.*, Nucl. Phys. **A531**, 453 (1991).
[17] D. Hahn and H. Stöcker, Nucl. Phys. **A452**, 723 (1986).
[18] A. Gobbi *et al.*, Nucl. Instrum. Methods Phys. Res., Sect. A **324**, 156 (1993).
[19] W. Reisdorf, in *Proceedings of the XX Workshop on Properties of Nuclei and Nuclear Excitation, Hirschegg, Austria, 1992* (GSI, Darmstadt, 1992).
[20] N. Herrmann, Nucl. Phys. **A553**, 739c (1993).
[21] T. Wienold, in Proceedings of NASI on Hot and Dense Nuclear Matter, Bodrum, Turkey, 1993, edited by W. Greiner and H. Stöcker, NATO ASI Ser. B (Plenum, New York, to be published).
[22] W. Reisdorf, in Proceedings of the XX Workshop on Properties of Nuclei and Nuclear Excitation (Ref. [19]).
[23] G. Fai and J. Randrup, Comput. Phys. Commun. **42**, 385 (1986).
[24] J. Randrup, Comput. Phys. Commun. **77**, 153 (1993).
[25] S.C. Jeong, in *Proceedings of the XXX International Winter Meeting on Nuclear Physics, Bormio, Italy, 1992*, edited by I. Iori (University of Milano, Milano, 1992).
[26] A. Bohnet *et al.*, Nucl. Phys. **A494**, 349 (1989).
[27] J.P. Coffin, in Proceedings of NASI on Hot and Dense Nuclear Matter (Ref. [21]).
[28] C. Kuhn *et al.*, Phys. Rev. C **48**, 1232 (1993).
[29] P. Danielewicz and Qiubao Pan, Phys. Rev. C **46**, 2002 (1992).

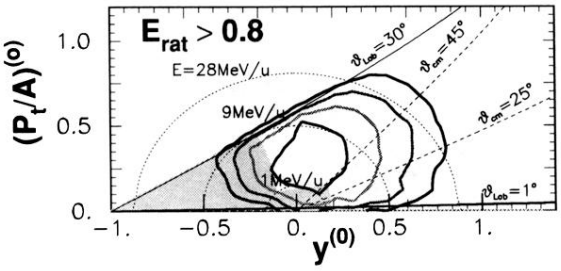

FIG. 1. Experimental rapidity plot for fragments with charge $3 \leq Z \leq 8$ for $E_{\rm rat} \geq 0.8$. Different fragments enter weighted with their respective element number. The contour lines represent cuts in invariant cross section (linear scale). The transverse momentum and rapidity scales are normalized as follows: $p_t^{(0)} = (p_t/A)/(p_{\rm pr}^{\rm c.m.}/A_{\rm pr})$ and $y^{(0)} = (y)/y_{\rm pr}^{\rm c.m.}$, respectively, where p_t and y are center-of-mass quantities; the index pr denotes projectile quantities. The solid lines indicate the detector boundary angles and the hatched area represents the energy threshold for $Z = 6$ products. The dotted circles denote constant energies per nucleon in the center of mass (1, 9, and 28A MeV, respectively).

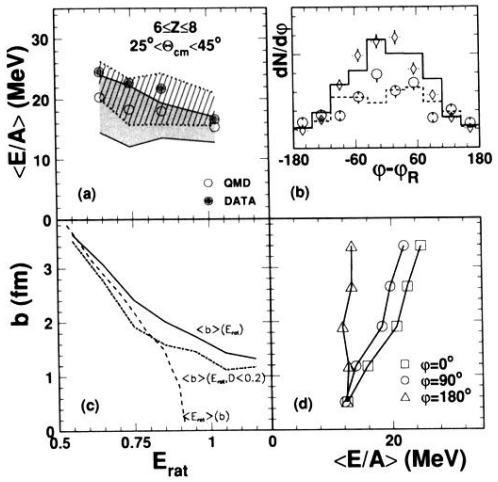

FIG. 3. Panel (a) shows for fragments with charges $6 \leq Z \leq 8$ the average kinetic energies in the angular range from 25° to 45°. Filled (open) circles represent data (QMD simulations [2]) at an azimuthal angle of $90° \pm 45°$ with respect to the reaction plane; the upper and lower borders of the hatched (shaded) area show the corresponding values at $0° \pm 45°$ and $180° \pm 45°$, respectively. Panel (b) displays for two $E_{\rm rat}$ bins, $0.7 < E_{\rm rat} < 0.8$ (solid line, diamonds) and $E_{\rm rat} > 0.9$ (dashed line, circles), the azimuthal distributions with respect to the reaction plane; histograms correspond to data, symbols to QMD simulations. Panel (c) shows the dependence of the average impact parameter as a function of $E_{\rm rat}$ (solid line), with an additional directivity cut (dash-dotted line), and the average $E_{\rm rat}$ as a function of the impact parameter (dashed line) within the QMD calculation. Panel (d) displays the average kinetic energies per nucleon as a function of the impact parameter and the azimuthal orientation within the QMD calculation.